Nikolay Ivanov Kolev

Multiphase Flow Dynamics

3 THERMAL INTERACTIONS

Fourth Edition

Springer

Multiphase Flow Dynamics 3

Nikolay Ivanov Kolev

Multiphase Flow Dynamics 3

Thermal Interactions

Springer

Author

Dr. Nikolay Ivanov Kolev
Möhrendorferstr. 7
91074 Herzogenaurach
Germany
E-mail: Nikolay.Kolev@herzovision.de

ISBN 978-3-642-21371-7 e-ISBN 978-3-642-21372-4

DOI 10.1007/978-3-642-21372-4

Library of Congress Control Number: 2011934250

Typeset & Cover Design: Scientific Publishing Services Pvt. Ltd., Chennai, India.

Printed on acid-free paper

9 8 7 6 5 4 3 2 1

springer.com

To Iva, Rali and Sonja with love!

Morning, July. 2004, Nikolay Ivanov Kolev, 36× 48cm oil on linen

Nikolay Ivanov Kolev, PhD, DrSc
Born 1.8.1951, Gabrowo, Bulgaria

Summary

This monograph contains theory, methods and practical experience for describing complex transient multiphase processes in arbitrary geometrical configurations. It is intended to help applied scientists and practicing engineers to understand better natural and industrial processes containing dynamic evolutions of complex multiphase flows. The book is also intended to be a useful source of information for students in the high semesters and in PhD programs.

This monograph consists of five volumes:

Vol. 1 Fundamentals, 4th edn, (14 Chapters and 2 Appendices), 782 pages;
Vol. 2 Mechanical Interactions, 4th edn, (11 Chapters), 364 pages;
Vol. 3 Thermal Interactions, 4th edn, (16 Chapters), 678 pages;
Vol. 4 Turbulence, Gas Absorption and Release by Liquid, Diesel Fuel Properties, 2nd edn, (13 Chapters), 328 pages;
Vol. 5 Nuclear Thermal Hydraulics, 2nd edn, (17 Chapters), 848 pages.

In Volume 1 the concept of three-fluid modeling is presented in detail "from the origin to the applications". This includes derivation of local volume- and time-averaged equations and their working forms, development of methods for their numerical integration and finally finding a variety of solutions for different problems of practical interest.

Special attention is paid in Volume 1 to the link between the partial differential equations and the constitutive relations called closure laws without providing any information on the closure laws.

Volumes 2 and 3 are devoted to these important constitutive relations for the mathematical description of the mechanical and thermal interactions. The structure of the volumes is in fact a state-of-the-art review and selection of the best available approaches for describing interfacial transfer processes. In many cases the original contribution of the author is incorporated in the overall presentation. The most important aspects of the presentation are that they stem from the author's long years of experience developing computer codes. The emphasis is on the practical use of these relationships: either as stand-alone estimation methods or within a framework of computer codes.

Volume 4 is devoted to the turbulence in multiphase flows.

The nuclear thermal hydraulic is the science providing knowledge about the physical processes occurring during the transferring the fission heat released in structural materials due to nuclear reactions into its environment. Along its way to

the environment the thermal energy is organized to provide useful mechanical work or useful heat or both. Volume 5 is devoted to the nuclear thermal hydraulics. In a way this is the most essential application of the multiphase fluid dynamics in analyzing steady and transient processes in nuclear power plants.

In particular, Volume 3 contains information on how to describe the flow patterns and the specific thermal interactions between the velocity fields in flight.

Chapter 1 presents nucleation in liquids. Chapter 2 presents different aspects of the bubble growth in superheated liquid and the connection to computational system models. Condensation of pure steam bubbles is considered in Chapter 3.

Chapter 4 considering the bubble departure mechanism on heated walls is updated with new information. The theory is extended to subcooled liquid.

Chapter 5 presents a solution of the coupled problem of transient bubble growth or collapse and relates it to the state-of-the-art. A comparison with experimental data is given. Finally, a discussion is provided on how to couple such low-scale physics with large-scale physics in multiphase flow computer codes.

Chapter 6 considering nucleate boiling is updated. Additional information coming from boiling of fluids with nanoparticles confirms the sound physical basics of the author's method. Additional information is provided for nucleation site density at high pressure.

An interesting result of the theory presented in these chapters is the prediction of a critical heat flux without an empirical correlation for critical heat flux as a result of the mutual bubble interaction for increasing wall superheating. Applying the theory for the inverted problem of the flashing of superheated water in pipes as given in Chapter 7, surprisingly supported the validity of the new approach.

The state-of-the-art in boiling theory is presented in Chapters 8 to 11 where boiling in subcooled liquid, natural convection film boiling, critical heat flux, forced convection film boiling, and film boiling on vertical plates and spheres is presented. The emphasis is on the elaboration of all coupling terms between the fluids, and between the wall and fluid required for closure of the overall description. Chapter 9 considering boiling of subcooled liquid is updated. Chapter 20 considering forced convection boiling is updated. The 2005 look-up table by *Groeneveld* et al. is demonstrated to be an excellent scaling base for critical heat flux in bundles for variety of geometries and conditions.

Chapter 12 provides information on all heat- and mass-transfer processes across a droplet interface starting with the nucleation theory, and going through the droplet growth, self-condensation stop, heat transfer across a droplet interface without mass transfer, direct contact condensation of pure steam on a subcooled droplet, spontaneous flushing of a superheated droplet, evaporation of a saturated droplet in superheated gas, and droplet evaporation in a gas mixture. A similar approach is applied to the description of the interface processes at a film/gas interface in Chapter 13 with a careful treatment of the influence of the turbulent pulsation on the interfacial heat and mass transfer. A set of updated empirical methods for prediction of condensation on cooled walls with and without a noncondensable

is presented in Chapter 14. Test examples are provided for demonstration of the application of the theory.

Chapter 15 provides information on the implementation of the discrete ordinate method for radiation transport in multiphase computer codes. In this chapter the dimensions of the problem, the differences between micro- and macrointeractions and the radiation transport equation are discussed. Then, the finite-volume representation of the radiation transport is given and different aspects of the numerical integration are discussed. The computation of some material properties is discussed. Then three specific radiation transport cases of importance for the melt–water interaction are discussed in detail: a spherical cavity of gas inside a molten material; concentric spheres of water droplets, surrounded by vapor surrounded by molten material; clouds of spherical particles of radiating material surrounded by a layer of vapor surrounded by water. For the last case the useful Lanzenberger's solution is presented and its importance is demonstrated in two practical cases.

The book ends with Chapter 16, which provides information on how to verify multiphase flow models by comparing them with experimental data and analytical solutions. First, Section 16.2 contains a quick look of the IVA computer code with several interesting demonstration of the power of the technology described in this four Volumes work. A list of references is provided in Sections 16.3 and 16.4 documenting the IVA-code development and validation. The complexity of the problems is gradually increased from very simple ones to problems with very complex melt–water interaction multifluid flows with dynamic fragmentation and coalescence and strong thermal and mechanical interactions. In particular the following cases are described and compared with the prediction using the basics presented in different chapters of this book: material relocation – gravitational waves (2D), U-tube benchmarks such us adiabatic oscillations, single-phase natural convection in a uniformly heated vertical part of a U-tube, single-phase natural convection in a uniformly heated inclined part of a U-tube, single-phase natural convection in a U-tube with an inclined part heated by steam condensation, steady-state single-phase nozzle flow, pressure waves in single-phase flow, 2D gas explosion in a space filled previously with gas, 2D gas explosion in space with internals previously filled with liquid, film entrainment in pipe flow, water flashing in nozzle flow, pipe blow-down with flashing, single-pipe transients, complex pipe network transients, boiling in pipes and rod bundles, critical heat flux, post-critical heat flux heat transfer, film boiling, behavior of clouds of cold and very hot spheres in water, experiments with dynamic fragmentation and coalescence like the FARO L14, 20, 24, 28, 31 experiments, PREMIX 13, 15, 17, 18 experiment, RIT and IKE experiment. Chapter 16 also contains some additional experiments and movies documenting the performance of the method for fast pressure wave propagation in 2D geometry and interesting acoustical problems of melt-water interaction. Review of the state-of-the-art of the instability analyses of boiling systems is provided and interesting comparison of the modern IVA predictions with large-scale AREVA- experiments is provided in Section 16.6.3. Powerful

demonstration of the methods for analyzing pressure-wave propagations in single- and two-phase systems is given by comparison with the Interatome experiments from 1983 performed on simple and complex pipe networks, Section 16.8.3. Section 16.15 contains comparison with 333 experiments for variety of bundles, flow regimes including dry out, steady state and transients. It clearly demonstrates the power of the method and its well-defined uncertainty to simulate boiling processes in complex geometry. In addition an application of a powerful method for investigation of the propagation of input and model uncertainties on the final results by using the Monte Carlo method and regression analysis is demonstrated for the prediction of nonexplosive melt-water interactions. Benchmarks for testing the 3D capabilities of computer codes are provided for the rigid-body steady-rotation problem, pure radial symmetric flow, radial-azimuthal symmetric flow. Examples of very complex 3D flows are also given such as small break loss of coolant, asymmetric steam–water interaction in a vessel, and melt relocation in a pressure vessel. And finally, Section 16.21 contains the discussion regarding: Is it possible to design a universal multiphase flow analyzer? It contains my personal vision for future development of the multiphase fluid dynamics.

Chapter 16 of this volume together with Chapter 14 of Volume 1 are available from the WEB site of Springer. In addition many animated sequences (movies) are presented there. HTML documents are then executed using any Web browser available on the local computer of the reader.

29.12.2010 Nikolay Ivanov Kolev
Herzogenaurach

Table of Contents

1. Nucleation in liquids

After reviewing the literature for description of the nucleation in superheated liquids the following conclusions and recommendations have been drawn. The maximum superheating in technical systems is a function of the depressurization velocity and of the produced turbulence. The maximum superheating can be predicted by the Algamir and Lienhard and by the Bartak correlations within an error band of 48.5%. Flashing in short pipes and nozzles leads to critical flows driven by the pressure difference equal to the entrance pressure minus the flashing inception pressure. For the prediction of the maximum achievable superheating, which represents the spinoidal line the Skripov correlation is recommended. The wetting angle is an important property of the polished surface characterizing its capability to activate nucleation sites. For the prediction of the activated nucleation sites the correlation obtained by Wang and Dhir is recommended. The establishing of a vapor film around a heated surface having temperature larger than the minimum film boiling temperature takes a finite time. The availability of small bubbles of noncondensing gases reduces the superheating required to initiate evaporation. Evaporation at lower than the saturation temperature is possible.

1.1 Introduction

Liquids having temperature above the saturation temperature corresponding to the local pressure are called superheated liquids. Superheated liquids are unstable and start to disintegrate. This process is in generally called *flashing*. The process of rupturing a *continuous* liquid by decrease in pressure at roughly constant liquid temperature is often called *cavitation* – a word proposed by *Froude*. The process of rupturing a *continuous* liquid by increase the temperature at roughly constant pressure is often called *boiling*. The fluctuation of molecules having energy larger than that characteristic of a stable state causes the formation of clusters of molecules, which after reaching some critical size are called nuclei. The theory of the nucleation provides us with information about the generation of nuclei per unit time and unit volume of the liquid as a function of the local parameter.

1.2 Nucleation energy, equation of *Kelvin* and *Laplace*

Let us abstract from a superheated *nonstable liquid a spherical volume*, having an initial radius R_{10}, a volume $\frac{4}{3}\pi R_{10}^3$, pressure p, temperature T_2 and density $\rho_2 = \rho_2(p, T_2)$. After some time the selected sphere liquid volume increases due to *evaporation* to the radius R_1 (respectively to the volume $\frac{4}{3}\pi R_1^3$) and reaches a pressure $p'(T_2)$. The pressure inside the bubble is assumed to be uniform because of the small bubble size. The density of the evaporated steam inside the sphere is $\rho'' = \rho''\left[p'(T_2)\right] = \rho''(T_2)$. The *initial* and the *end spheres have the same mass* per definition, therefore

$$\left(\frac{R_{10}}{R_1}\right)^3 = \frac{\rho''}{\rho_2}. \tag{1.1}$$

Consequently, the initial volume of the sphere is changed by

$$\frac{4}{3}\pi\left(R_1^3 - R_{10}^3\right) = \frac{4}{3}\pi R_1^3\left(1 - \frac{\rho''}{\rho_2}\right). \tag{1.2}$$

During this expansion a *mechanical work*

$$4\pi\int_{R_{10}}^{R_1}\left[p'(T_2) - p\right]r^2 dr \approx \frac{4}{3}\pi\left(R_1^3 - R_{10}^3\right)\left[p'(T_2) - p\right]$$

$$= \frac{4}{3}\pi R_1^3\left(1 - \frac{\rho''}{\rho_2}\right)\left[p'(T_2) - p\right] \tag{1.3}$$

is performed and transferred into total kinetic energy of the surrounding liquid *Skripov* et al. (1980). In other words, this work is introduced into the liquid. For the creation of a sphere with a free surface, additional work

$$\int_0^{R_1}\frac{2\sigma}{r}4\pi r^2 dr = 4\pi R_1^2\sigma \tag{1.4}$$

is needed. The surface tension of water in N/m, σ, in contact with its vapor is given in *Lienhard* (1976) with great accuracy by

$$\sigma = 0.2358\left[1 - \frac{T'(p)}{T_c}\right]^{1.256}\left\{1 - 0.625\left[1 - \frac{T'(p)}{T_c}\right]\right\}, \tag{1.5}$$

where the T_c is the thermodynamic critical temperature (for water T_c = 647.2 K). For the region of 366 to 566 K the above equation can be approximated by

$$\sigma = 0.14783\left(1 - T/T_c\right)^{1.053} \tag{1.6}$$

with an error of $\pm 1\%$. The surface tension is a function of the surface temperature, which can strongly vary in transients. The surface tension is usually measured at macroscopic surfaces. Whether the so-obtained information is valid for the microscopic metastable bubbles is not clear. Next, we assume that this relationship holds also for microscopic surfaces.

Thus, the work necessary to create a single bubble with radius R_1 is

$$\Delta E_1 = 4\pi R_1^2 \sigma - \left[p'(T_2) - p\right]\frac{4}{3}\pi R_1^3\left(1 - \frac{\rho''}{\rho_2}\right) = 4\pi\sigma\left(R_1^2 - \frac{2}{3}\frac{R_1^3}{R_{1c}}\right),\ p'(T_2) > p \tag{1.7}$$

We see that this work depends on the bubble radius and has a maximum

$$\Delta E_{1c} = \frac{16\pi\sigma^3}{3\left[p'(T_2) - p\right]^2\left(1 - \frac{\rho''}{\rho_2}\right)^2} = \frac{4}{3}\pi\sigma R_{1c}^2 \approx \frac{4}{3}\pi\sigma\left[\frac{T'(p)}{T_2 - T'(p)}\frac{2\sigma}{\rho''(h'' - h')}\right]^2 \tag{1.8}$$

for

$$R_{1c}^2 = \frac{3\Delta E_{1c}}{\sigma 4\pi} = \left\{\frac{2\sigma}{\left[p'(T_2) - p\right]\left(1 - \rho''/\rho_2\right)}\right\}^2. \tag{1.9}$$

The corresponding bubble volume is then

$$V_{1c} = \frac{4}{3}\pi\left(\frac{3\Delta E_{1c}}{\sigma 4\pi}\right)^{3/2}. \tag{1.10}$$

The equation (1.9) is known as the *Laplace* and *Kelvin* equation. *Gibbs* (1878) noted that the expression for the maximum " ... does not involve any geometrical magnitudes".

1.3 Nucleus capable of growth

The above consideration did not lead to any conclusion whether a bubble with size R_{1c} will further grow or collapse. It says only that at that size the mechanical energy needed to create a bubble at the initial state $R_1 = 0$ and at the final state $R_{1\infty} > R_{1c}$ possesses a maximum at R_{1c} and no more. There are many papers in which this size is taken to represent the bubble size, at which the bubble is further capable to grow, which as we will show below is not true.

Next, we consider the conservation of the liquid mechanical energy in order to describe the bubble growth from the beginning through the critical radius. The mass-conservation equation of the liquid can be approximated by

$$\frac{1}{r^2}\frac{\partial}{\partial r}\left(r^2 u_2\right) \approx 0, \tag{1.11}$$

or integrating with the boundary condition

$$r = R_1, \quad u_2 = \frac{\partial R_1}{\partial \tau} \tag{1.12}$$

$$u_2 = const / r^2 = \frac{\partial R_1}{\partial \tau}\left(R_1 / r\right)^2. \tag{1.13}$$

This gives the liquid velocity as a function of the radius if the liquid is assumed to be incompressible during the bubble expansion. The total kinetic energy of the liquid environment estimated using the above equation is therefore

$$\int_{R_1}^{\infty} \frac{1}{2}\rho_2 u_2^2 dVol_2 = \frac{1}{2}\rho_2 \left(\frac{\partial R_1}{\partial \tau}\right)^2 R_1^4 4\pi \int_{R_1}^{\infty} \frac{dr}{r^2} = 2\pi\rho_2 \left(\frac{\partial R_1}{\partial r}\right)^2 R_1^4 \int_{R_1}^{\infty} d\left(-\frac{1}{r}\right)$$

$$= 2\pi\rho_2 \left(\frac{\partial R_1}{\partial \tau}\right)^2 R_1^3. \tag{1.14}$$

During the bubble growth, the work performed by the bubble expansion is transferred in total kinetic energy of the liquid environment, i.e.,

$$2\pi\rho_2 \left(\frac{\partial R_1}{\partial \tau}\right)^2 R_1^3 = -4\pi\sigma\left(R_1^2 - \frac{2}{3}\frac{R_1^3}{R_{1c}}\right) \equiv \Delta E_1$$

or

$$\left(\frac{\partial R_1}{\partial \tau}\right)^2 = \frac{2\sigma}{\rho_2}\left(\frac{2}{3}\frac{1}{R_{1c}} - \frac{1}{R_1}\right). \tag{1.15}$$

The constant 2/3 valid for bubble growth in a bulk liquid should be replaced by $\pi/7$ if a spherical bubble grows on a flat surface.

Equation (1.15) is a very important result. We see that real bubble growth is possible *if and only if*

$$R_1 > \frac{3}{2} R_{1c}. \tag{1.16}$$

For the case of $R_1 >> R_{1c}$ Eq. (1.15) transforms into

$$\left(\frac{\partial R_1}{\partial \tau}\right)^2 = \frac{4}{3}\frac{\sigma}{\rho_2 R_{1c}}. \tag{1.17}$$

This mechanism of bubble growth is called *inertially controlled bubble growth*. For low pressure where the assumption $\rho''/\rho_2 = 0$ is reasonable the above equation reduces to one obtained for the first time by *Besand* (1859) and in a more elegant way by *Rayleigh* (1917). This mechanism controls the bubble growth within the first 10^{-8} s of the life of the stable bubble.

It follows from the above consideration that for the creation of a bubble with a critical unstable diameter 3/2 R_{1c}, a surplus of internal energy of the liquid is needed greater than E_{1c}, and for creation of bubble that is capable to grow, a surplus of internal energy of the liquid – greater than (9/4) E_{1c}.

1.4 Some useful forms of the *Clausius–Clapeyron* equation, measures of superheating

Usually, the liquid superheating is expressed by the temperature difference $T_2 - T'(p)$. Sometimes, the pressure difference $\Delta p = p'(T_2) - p$ corresponding to the superheating of the liquid with respect to the saturation temperature $T_2 - T'(p)$ is also used as a measure for the liquid superheating. Using the *Clausius–Clapeyron* equation

$$\frac{dT}{dp} = \frac{v'' - v'}{s'' - s'} = \frac{\rho' - \rho''}{s'' - s'}\frac{1}{\rho'\rho''} = T'(p)\frac{\rho' - \rho''}{h'' - h'}\frac{1}{\rho'\rho''} \tag{1.18}$$

integrated between the initial state [p, $T'(p)$] and the final state [$p'(T_2)$, T_2] for

$$\frac{\rho' - \rho''}{h'' - h'}\frac{1}{\rho'\rho''} \approx const \tag{1.19}$$

one obtains

$$p'(T_2) - p = \left(h'' - h'\right)\frac{\rho'\rho''}{\rho' - \rho''}\ln\left[1 + \frac{T_2 - T'(p)}{T'(p)}\right]. \tag{1.20}$$

With this result the critical bubbles size can be approximated by

$$R_{1c} \approx 2\sigma / \left\{(h'' - h')\rho' \ln\left[1 + \frac{T_2 - T'(p)}{T'(p)}\right]\right\}. \tag{1.22}$$

For $T_2 - T'(p) << T'(p)$ we have for the tensile pressure difference

$$p'(T_2) - p = \left(h'' - h'\right) \frac{\rho'\rho''}{\rho' - \rho''} \frac{T_2 - T'(p)}{T'(p)}, \tag{1.23}$$

and for the critical bubble size

$$R_{1c} \approx \frac{T'(p)}{T_2 - T'(p)} \frac{2\sigma}{\rho''(h'' - h')}. \tag{1.24}$$

Thus, one can use as a measure of liquid superheating either the *tension pressure difference* $p'(T_2) - p$ or the *liquid superheat* $T_2 - T'(p)$.

Equation (1.23) makes it possible to compute the liquid superheating corresponding to the radius R_{1c} from Eq. (1.9)

$$\left[T_2 - T'(p)\right] / T'(p) = \frac{2\sigma}{R_{1c}} \frac{(\rho' - \rho'')\rho_2}{(\rho_2 - \rho'')\rho'\rho''} \frac{1}{h'' - h'} \approx 2 \frac{\sigma}{R_{1c}} \frac{1}{\rho''\left(h'' - h'\right)} \tag{1.25}$$

or corresponding to 3 R_{1k}/2

$$\left[T_2 - T'(p)\right] / T'(p) = \frac{4}{3} \frac{\sigma}{R_{1c}} \frac{(\rho' - \rho'')\rho_2}{(\rho_2 - \rho'')\rho'\rho''} \frac{1}{h'' - h'} \approx \frac{4}{3} \frac{\sigma}{R_{1c}} \frac{1}{\rho''\left(h'' - h'\right)}. \tag{1.26}$$

For the atmospheric pressure Eq. (1.23) gives

$$T_2 - T'(p) = 6.4197 \times 10^{-5} / D_{1c}. \tag{1.27}$$

This linearization is valid for very small deviations from the saturation. In general, the participating properties are not a linear function of temperature. A nonlinear expression is obtained also for low pressure for which the density difference between liquid and vapor is very large. In this case Eq. (1.18) simplifies to $dT/dp = v''/\left(T\Delta h\right)$. This equation has been known since 1828 in France as the *August* equation. Assuming the vapor behave as a perfect gas results in $dp/p = \left(\Delta h/R\right) dT/T^2$, where R is the vapor gas constant for the specific substance. Integrating between an initial state [p, $T'(p)$] and a final state [$p'(T_2)$, T_2] and rearranging results in useful expression for computing the relation between *tension pressure difference* $p'(T_2) - p$ and the *liquid superheat* $T_2 - T'(p)$ of metastable liquid,

$$\frac{p'\left(T_2\right) - p}{p} = \exp\left[\frac{\Delta h}{RT_2} \frac{T_2 - T'\left(p\right)}{T'\left(p\right)}\right] - 1. \tag{1.28}$$

With this result the *Laplace* and *Kelvin* equation reads

$$R_{1c} \approx \frac{2\sigma}{\left\{\exp\left[\frac{\Delta h}{RT_2} \frac{T_2 - T'\left(p\right)}{T'\left(p\right)}\right] - 1\right\} p\left(1 - \rho''/\rho_2\right)}. \tag{1.29}$$

One should carefully use the approximations of the *Laplace* and *Kelvin* equation. At low pressure the approximations are good as shown in Fig.1.1. In this case at higher superheat Eq. (1.29) is much closer to the accurate equation.

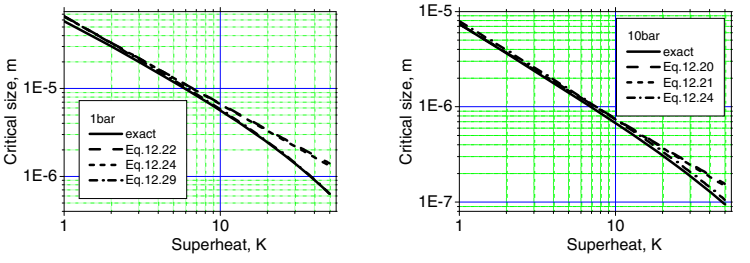

Fig. 1.1 Critical bubbles size at low pressure as a function of the liquid superheat

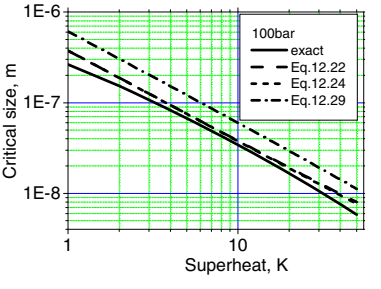

Fig. 1.2 Critical bubbles size at high pressure as a function of the liquid superheat

At high pressure the approximations may deviate substantially from the exact solution as shown in Fig. 1.2.

The dimensionless number constructed as follows

$$Gb_2 = \frac{\Delta E_{1c}}{kT_2} = \frac{\Delta S_{1c}}{k} = \frac{16\pi\sigma^3}{kT_2 3\left[p'(T_2) - p\right]^2 \left(1 - \rho''(T_2)/\rho_2\right)^2} \tag{1.30}$$

is called the *Gibbs* number. Here, $k = 13.805\times10^{-24}$ J/K is the *Boltzmann* constant. The *Gibbs* number is frequently used as a dimensionless measure of superheating. The greater the superheating the smaller the *Gibbs* number. Gb_2 converging to infinity means no superheating. For $T_2 = T_c$, $\sigma = 0$ and $Gb_2 = 0$.

However, it should be noted that neither of the measures discussed above tells us at what ΔT liquid starts boiling or flashing.

1.5 Nucleation kinetics

1.5.1 Homogeneous nucleation

Now we discuss the dependence between liquid superheating and production rates of bubbles with critical size called nuclei. Consider a continuous liquid characterized by average state parameters p and T_2. An observer measures a long time $\Delta\tau$ the time $\Delta\tau_n$ in which a mass Δm_{2c} of the continuum departs from the normal, average, state. The entropy change necessary for this fluctuation is $\Delta m_{2c}\Delta s_{2c} = \Delta S_{2c}$. *Volmer* (1939) p. 81 following *Boltzmann* and *Einstein* assumed that

$$\Delta\tau_n / \Delta\tau \approx const\ \mathrm{e}^{-\Delta S_{2c}/k} = const\ e^{-Gb_2} \tag{1.31}$$

where k is the *Boltzmann* constant. This means that the smaller the needed entropy change for the fluctuation the higher the probability of this fluctuation. This is the leading idea for describing such processes. It did not change with the years. Actually it is known from experimental observations that the greater the superheating the greater the probability of initiation of bubbles with critical size. The probability of initiation of a single bubble is defined as

$$\text{probability of initiation of single bubble} = \frac{nucleation\ \ events}{molecular\ \ colisions}. \tag{1.32}$$

Thus,

$$\frac{nucleation\ \ events}{molecular\ \ colisions} = \exp(-Gb_2) \tag{1.33}$$

Obviously for $T_2 = T_c$ and $\sigma_2 = 0$, the probability of initiation of a single bubble $exp(-Gb_2) = 1$. Nuclei with critical size can originate in the bulk liquid. This phenomenon is called *homogeneous* nucleation. Nuclei with critical size can originate also at the wall. This phenomenon is called *heterogeneous* nucleation. The theories modeling the nucleation in the bulk liquid are called homogeneous nucleation theories. The theories modeling the nucleation at surfaces are called heterogeneous nucleation theories. Next, we give the main result of the homogeneous nucleation theory.

Kaishew and *Stranski* computed in 1934 the number of the created nuclei per unit time in unit volume of the liquid as follows

$$\dot{n}_{1cin} = N_2 \left\{ \frac{6\sigma}{\left[2 + p/p'(T_2)\right]\pi\ m_2} \right\}^{1/2} \exp(-Gb_2)$$

$$= \exp\left\{ \ln\left[\rho_2 \left(\frac{N_A}{m_\mu} \right)^{3/2} \left\{ \frac{6\sigma}{\left[2 + p/p'(T_2)\right]\pi\ m_2} \right\}^{1/2} \right] - Gb_2 \right\}. \tag{1.34}$$

Here, $N_2 = \rho_2/m_2 = \rho_2 N_A/m_\mu$ (≈ 3.3–10^{28} for water) is the number of the molecules in one cubic meter, $m_2 = m_\mu/N_A$ is the mass of a single molecule, m_μ is the kg-mole mass (18 *kg* for water), $N_A = 6.02\times 10^{26}$ (1/kg-mole) is the number of molecules in one kilogram-mole mass, the *Avogadro* number, and

$$\left\{\frac{6\sigma}{\left[2+p/p'(T_2)\right]\pi m_2}\right\}^{1/2} \tag{1.35}$$

is the frequency with which each single liquid molecule interacts with its neighbors. The logarithmic expression is not very sensitive with respect to p and T_2 and ranges over

$$\ln\left[\rho_2\left(\frac{N_A}{m_\mu}\right)^{3/2}\left\{\frac{6\sigma}{\left[2+p/p'(T_2)\right]\pi m_2}\right\}^{1/2}\right] \approx 80 \; to \; 83 \tag{1.36}$$

for water.

1.5.2 Heterogeneous nucleation

1.5.2.1 Characteristics of the surfaces and of the liquid/surface contact

Technical surfaces possess roughness as a result of the manufacturing procedure. The structure of the roughness is an important characteristic of the nucleation processes at the surface. Another important characteristic is the molecular interaction between the surface and the liquid. It is usually characterized by the so-called contact angle. The angle between the tangent to the interface and the wall θ is called the contact angle. Hydrophobic surfaces, $\theta > 0$, cause heterogeneous nucleation at much reduced pressure difference (tensile strength). In this section, we give some examples of the characteristics of surfaces influencing the heterogeneous nucleation kinetics.

At real surfaces there are several cavities. For ordinary machined surfaces the cavities have sizes from 2 to 6 μm with density in the range of

$$n_w'' \approx (10 \; to \; 250)\times 10^4 m^{-2} \tag{1.37}$$

For mirror finished copper surfaces as described in *Wang and Dhir* (1993) physically existing cavities have been found to have surface densities depending on the equivalent cavity size in the range

$$n_w'' \approx 9\times 10^{-9}/D_{cav}^2 \quad \text{for} \quad D_{\text{cav}} \geq 5.8\times 10^{-6} m \tag{1.38}$$

$$n_w'' \approx 10.3\times 10^4 + 1.5\times 10^{-25.2}/D_{cav}^{5.2} \quad \text{for} \quad 3.5\times 10^{-6} \leq D_{\text{cav}} \leq 5.8\times 10^{-6} m \tag{1.39}$$

$$n''_w \approx 2.2135\times10^7 + 3.981\times10^{-26.4} / D_{cav}^{5.4} \quad \text{for} \quad D_{\text{cav}} \le 3.5\times10^{-6} m \,. \qquad (1.40)$$

These are surface properties, which depend on the surface manufacturing only. The authors discovered that only cavities having a nearly spherical form and mouth angle less than the static contact angle serve as nucleation sites. The mouth angle is the angle between the boiling surface and the internal surface of the cavity forming the mouth. The region of changing the heat flux covers the entire nucleate boiling region.

The following tables give some information on how the contact angle can change for different wall materials and different surface preparation procedures.

Table 1.1 Static contact angles θ for distilled water at polished surfaces.

Steel	$\pi/3.7$	*Siegel* and *Keshock* (1964)
Steel, Nickel	$\pi/4.74$	*Bergles* and *Rohsenow* (1964)
Nickel	$\pi/4.76$ to $\pi/3.83$	*Tolubinsky* and *Ostrovsky* (1966)
Nickel	$\pi/4.74$ to $\pi/3.83$	*Siegel* and *Keshock* (1964)
Chrome-Nickel Steel	$\pi/3.7$	*Arefeva* and *Aladev* (1958)
Silver	$\pi/6$ to $\pi/4.5$	*Labuntsov* (1963) for p =1 to 150 bar
Zinc	$\pi/3.4$	*Arefeva* and *Aladev* (1958)
Bronze	$\pi/3.2$	*Arefeva* and *Aladev* (1958)
Zr-4	$\pi/3.16$	*Basu*, et al. (2002)
Note the contradictory data for copper in the literature		
Copper	$\pi/4$	*Arefeva* and *Aladev* (1958)
Copper	$\pi/3$	*Gaertner* and *Westwater* (1960)
Copper	$\pi/2$	*Wang* and *Dhir* (1993)
Stainless steel 304 (25 °C)	$\theta_{25} \approx \pi/2.25$	*Hirose* et al. (2006)
Zircaloy (25 °C)	$\theta_{25} \approx \pi/2.46$	*Hirose* et al. (2006)
Aluminum (25 °C)	$\theta_{25} \approx \pi/2$	*Hirose* et al. (2006)

Table 1.2 Static contact angle θ for distilled water at thermally or chemically treated polished surfaces

Copper heated to 525 K and exposed to air one hour:	$\pi/5.14$	*Wang* and *Dhir* (1993)
Copper heated to 525 K and exposed to air two hour:	$\pi/10$	*Wang* and *Dhir* (1993)
Chrome-Nickel Steel chemically treated:	$\pi/2.9$	*Arefeva* and *Aladev* (1958)

Hirose et al. (2006) found that the wetting angle is a function of the wall temperature. He correlated measurements within $\pm 12.5\%$ uncertainty band for nitrogen and argon and water–stainless steel 304, water–zircaloy and water–aluminum for pressures 1 to 151 bar and temperatures 20 to 300 °C by the expression

$$\theta = \theta_{25} \tanh\left(2.55 \times T^{*1.72}\right) \text{ for } T^* > 0.3,$$

$$\theta = \theta_{25} \tanh\left(2.55 \times 0.3^{1.72}\right) \text{ for } T^* < 0.3,$$

where $T^* = \dfrac{T_{cr} - T_w}{T_{cr} - (273.15 + 25)}$, T_{cr} is the critical water temperature and T_w is the wall temperature and $\theta_{25} = \theta\left(25°C\right)$. Note that there is no zero wettability at the critical temperature. This is important finding. The work by *Hirose* et al. (2006) shows that measurements for wetting angles can be compared to each other if they are made at the same wall temperature.

In the case of nucleation at walls the segment of a bubble attached at the cavity possesses

$$\textit{surface area} = \varphi 4\pi R_{1c}^2, \tag{1.41}$$

which is less than the nucleation surface by a factor of φ. Therefore, less energy is needed for the creation of bubbles at walls

$$\Delta E_{1c}^* = \varphi \Delta E_{1c}, \tag{1.42}$$

than inside the liquid. Consequently, the superheating that can be achieved in technical systems is much smaller than in spontaneous bulk nucleation systems. φ is frequently called the work-reduction factor in the literature.

Tolubinski (1980) computed the work-reduction factor, φ, for an idealized wall surface having *plane geometry* without cavities as follows

$$\varphi = \frac{1}{4}\left(1 + \cos\theta\right)^2 \left(1 - \cos\theta\right). \tag{1.43}$$

Using the values from Table 1.1 we have φ s in the range of 0.078 to 0.25.

The work-reduction factor for surface with cavities calculated by *Kottowski* (1973) is

$$\varphi = \frac{1}{4}\left[2 - 3\sin(\theta - \Phi) + \sin^3(\theta - \Phi)\right]. \tag{1.44}$$

Here, Φ is the cavity angle if the cavity is idealized as a cone.